Received: 17 September 2020 | Revised: 10 December 2020 | Accepted: 14 December 2020

DOI: 10.1002/bit.27658

ARTICLE

BIOTECHNOLOGY AND BIOENGINEERING WILEY

Introduction of glycine synthase enables uptake of exogenous formate and strongly impacts the metabolism in *Clostridium pasteurianum*

Yaeseong Hong[1] | Philipp Arbter[1] | Wei Wang[1] | Lilian N. Rojas[1] | An-Ping Zeng[1,2]

[1]Institute of Bioprocess and Biosystems Engineering, Hamburg University of Technology, Hamburg, Germany

[2]Beijing Advanced Innovation Center for Soft Matter Science and Engineering, Beijing University of Chemical Technology, Beijing, China

Correspondence

Yaeseong Hong and An-Ping Zeng, Institute of Bioprocess and Biosystems Engineering, Hamburg University of Technology, Denickestraße 15, Hamburg 21073, Germany.
Email: yaeseong.hong@tuhh.de (Y. H.) and aze@tuhh.de (A.-P. Z.)

Abstract

Autotrophic or mixotrophic use of one-carbon (C1) compounds is gaining importance for sustainable bioproduction. In an effort to integrate the reductive glycine pathway (rGP) as a highly promising pathway for the assimilation of CO_2 and formate, genes coding for glycine synthase system from *Gottschalkia acidurici* were successfully introduced into *Clostridium pasteurianum*, a non-model host microorganism with industrial interests. The mutant harboring glycine synthase exhibited assimilation of exogenous formate and reduced CO_2 formation. Further metabolic data clearly showed large impacts of expression of glycine synthase on the product metabolism of *C. pasteurianum*. In particular, 2-oxobutyrate (2-OB) was observed for the first time as a metabolic intermediate of *C. pasteurianum* and its secretion was solely triggered by the expression of glycine synthase. The perturbation of C1 metabolism is discussed regarding its interactions with pathways of the central metabolism, acidogenesis, solventogenesis, and amino acid metabolism. The secretion of 2-OB is considered as a consequence of metabolic and redox instabilities due to the activity of glycine synthase and may represent a common metabolic response of Clostridia in enhanced use of C1 compounds.

KEYWORDS

Clostridium pasteurianum, formate assimilation, glycine synthase

1 | INTRODUCTION

Utilization of one-carbon compounds such as CO_2, formate, or methanol as alternative carbon sources for biosynthesis has gained large interest recently. In the past few years, approaches of using *Escherichia coli* as a host for engineering have generated various synthetic biology examples of introducing C1-assimilation pathways, resulting in full autotrophy and reaching comparable cell densities to sugar-based cultivations (Bang et al., 2020; Gleizer et al., 2019). Among others, the most accessible pathways are the reductive glycine pathway (rGP), the ribulose monophosphate pathway, and the Calvin–Benson–Bassham cycle (see reviews for deeper analysis: Antoniewicz, 2019; Cotton et al., 2019; Mao et al., 2020; Tuyishime and Sinumvayo, 2020). Further studies focused on alternative organisms, such as *Saccharomyces cerevisiae* (Dai et al., 2017; Gonzalez de la Cruz et al., 2019), *Pichia pastoris* (Gassler et al., 2020),

Desulfovibrio desulfuricans (Sánchez-Andrea et al., 2020), *Cupriavidus necator* (Claassens et al., 2020), and *Corynebacterium glutamicum* (Hennig et al., 2020; Tuyishime et al., 2018; Witthoff et al., 2015). For the most studied *Clostridia*, namely *Clostridium acetobutylicum*, foundations for the utilization of the reductive acetyl-CoA pathway (rAP) were laid by studying the expression and activity of acetyl-CoA synthase (Carlson & Papoutsakis, 2017; Fast & Papoutsakis, 2018). In general, however, non-model microorganisms have received less attention in the effort of integration of C1-utilization pathways mostly due to the lack of genetic tools, and probably also the less competitiveness compared with using native C1-fixating microorganisms.

Our long-term goal is to construct an anaerobic heterotrophic strain capable of synthesizing valuable chemicals with carbons derived from fixated C1 compounds and nitrogen from molecular nitrogen, in combination with energy and electrons derived from inexpensive waste materials, such as raw glycerol, even partially from electric currents. In this regard, *Clostridium pasteurianum*, a gram-positive, anaerobic, endospore-forming, and molecular nitrogen fixating bacterium with excellent solvent producing properties, was chosen to be engineered into a C1-utilizing model strain. For metabolic engineering of *C. pasteurianum*, one of the largest challenges lies in its low transformation efficiency. Although an in vivo methylation and electro-transformation protocol based on Pyne et al. (2013) was established, and *C. pasteurianum* R525 with improved electro-competence was isolated in our laboratory (Schmitz et al., 2019), transformation of several variations of pMTL-based plasmids failed in follow-up studies (data not shown). While the reason for the transformation failure remains unclear, we observed that smaller plasmids, such as pMTL85141 as a non-expression plasmid (Heap et al., 2009), were able to yield higher transformation efficiencies. Thus, it was reasonable to assume that chances of being rejected by the host strain due to restriction-modification system or other sequence-specific incompatibilities might be reduced by minimizing the plasmid size and complexity. Therefore, we approached meeting the criteria of simplicity and compliance with the native cellular machinery, using a design based on the principle of orthogonality (Pandit et al., 2017).

Comparing natural and synthetic C1-assimilation pathways, the reductive glycine pathway schemed in Figure 1 represents a very promising one (Bar-Even, 2016; Bar-Even et al., 2013). Genomic analysis of genes required by rGP revealed that glycine synthase (or glycine cleavage system) is the only missing reaction step in *C. pasteurianum*. Comprised of four proteins (T, H, P, and L) the glycine synthase converts 5,10-methylene-THF, CO_2, NH_3, and NADH to glycine (Kikuchi et al., 2008). Interestingly, many species among the well-known *Clostridia* lack the glycine synthase/glycine cleavage system (Table S1). This makes them suitable candidates to investigate the effects in a neutral and orthogonal manner without

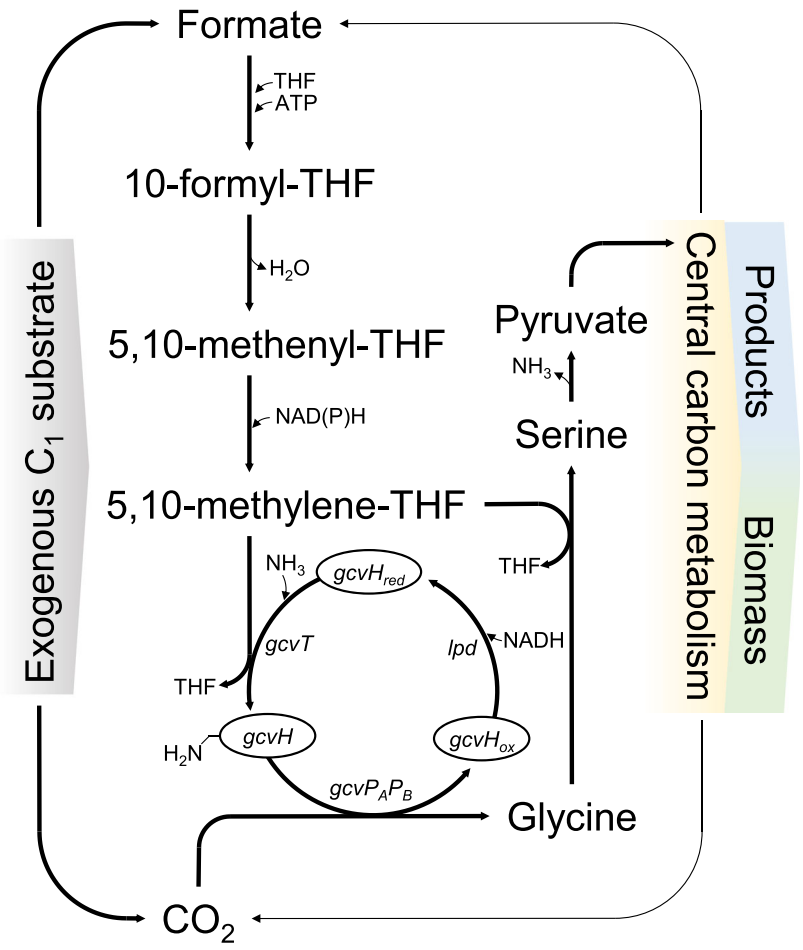

FIGURE 1 Reductive glycine pathway and sources of formate and CO_2 for *Clostridium pasteurianum*. Formate is assimilated through the partial folate cycle and enters the glycine synthase in a reduced state. Tetrahydrofolate (THF) acts as a carrier of C1-unit and provides two of the three C1 units for the reductive glycine pathway, while the third carbon is derived from CO_2. Glycine synthase as a reverse operating glycine cleavage system (*gcvT*: aminomethyltransferase, T-protein; $gcvP_AP_B$: glycine dehydrogenase, P-protein; *lpd*: dihydrolipoyl dehydrogenase; L-protein, *gcvH*: H-protein) converts 5,10-methylene-THF, NH_3, and CO_2 to glycine, which is further converted to serine via serine hydroxymethyltransferase. After deamination of serine, one molecule of pyruvate is generated, which is further channeled into the central metabolic pathways or into biomass [Color figure can be viewed at wileyonlinelibrary.com]

interference through a parallel reaction system. As an effort to integrate rGP in *C. pasteurianum*, genes of the glycine synthase from *Gottschalkia acidurici* (f. *Clostridium acidurici*; Poehlein et al., 2017) were chosen, because it is one of the few organisms operating the glycine synthase natively in the direction of glycine synthesis (Gariboldi & Drake, 1984; Waber & Wood, 1979). In this study, genes of glycine synthase from *G. acidurici* were cloned and introduced into *C. pasteurianum*, which was then characterized using glycerol, glucose, and formate as feed compounds. By comparing the mutant with the wild-type strain under variation of cultivation conditions, the metabolic impact of introducing glycine synthase into *C. pasteurianum* was addressed.

2 | MATERIALS AND METHODS

2.1 | Chemicals

Agarose was purchased from Biozyme Scientific GmbH and molecular nitrogen from Westfalen AG. ^{13}C labeled sodium formate (99%) from Sigma-Aldrich/Merck was used for ^{13}C-labeling experiments. All the other chemicals of analytical grade were purchased either from Carl Roth or from Sigma-Aldrich/Merck.

2.2 | Strains and plasmids

Strains and plasmids used in this study are listed in Table 1. Primers and their purpose are described in Table 2. For plasmid construction, propagation, and in vivo methylation, *E. coli* 10β (New England Biolabs) was used. Polymerase chain reaction (PCR) was performed with CloneAmp HiFi PCR Premix (Takara Bio Inc.) with primers purchased from Thermo Fisher Scientific. For PCR products with templates originated from *E. coli*, FastDigest DpnI (Thermo Fisher Scientific) was used. In-Fusion Cloning (Takara Bio Inc.) was used for the construction of the pMTL-GCSY1 plasmid: *gcvT* (Curi_c00740), *gcvH* (Curi_c00750), $gcvP_AP_B$ (Curi_c00760 and Curi_c00770), and *lpd* (Curi_c09790) from genomic DNA of *G. acidurici* DSM 604 and pMTL-vector backbone from pMTL85141-Cas9n (Schmitz et al., 2019) were PCR amplified and cloned, yielding in pMTL-GCSY1. Colony-PCR was performed with Maxima Hot Start PCR Master Mix (Thermo Fisher Scientific) and the resulting plasmid was sequenced externally via Sanger sequencing (Microsynth Seqlab). NucleoSpin and NucleoBond Plasmid kits and NucleoSpin Gel and PCR Clean-up (Macherey-Nagel) were used for plasmid DNA extraction and purification of DNA. For purchased kits, manufacturers' protocols were followed. DNA concentrations were measured by NanoDrop One (Thermo Fisher Scientific).

2.3 | Media, growth conditions, and storage of bacteria

E. coli strains were stored in Roti-Store cryo vials (Carl Roth) and cultivations were performed in LB medium (tryptone, 10 g L^{-1}; yeast extract, 5 g L^{-1}; NaCl, 5 g L^{-1}) at 37°C in 50 ml conical tubes or Erlenmeyer flasks with baffles. If required, additional 1.5% (w/v) agar was added. For selection, chloramphenicol and kanamycin were supplemented to final concentrations of 25–34 μg ml^{-1} and 35–50 μg ml^{-1}, respectively.

C. pasteurianum strains were stored at −80°C as 20% (v/v) glycerol stocks in 1.8 ml cryovials (VWR). For cultivation, glycerol stocks were first inoculated to serum bottles containing 2 × YTG medium (tryptone, 16 g L^{-1}; yeast extract, 10 g L^{-1}; glucose, 5 g L^{-1}; Pyne et al., 2013), grown at 35°C for 12–40 h, then transferred to modified Biebl medium and grown at 35°C. The basal Biebl medium

TABLE 1 Strains and plasmids used in this study

Name	Description	Source
Strains		
E. coli 10β	*Δ(ara-leu) 7697 araD139 fhuA ΔlacX74 galK16 galE15 e14- ϕ80dlacZΔM15 recA1 relA1 endA1 nupG rpsL* (Str^R) *rph spoT1 Δ(mrr-hsdRMS-mcrBC)*	New England Biolabs
C. pasteurianum R525	Isolated *C. pasteurianum* DSM 525 clone with enhanced transformation efficiency	Schmitz et al. (2019)
Genomic DNA from *Gottschalkia aicurici* DSM 604	Source of studied glycine synthase of this study	DSMZ
Plasmids		
pMTL85141-Cas9n	Shuttle vector (*E. coli* and *C. pasteurianum*) expressing Cas9 nickase under fdx promotor originated from *Clostridium sporogenes* (Cm^R; ColE1 ori; pIM13 ori)	Schmitz et al. (2019)
pFnuDIIMKn	In vivo methylation plasmid for *E. coli* via FnuDII methyltransferase from *Fusobacterium nucleatum* (p15A ori; Kn^R)	Pyne et al. (2013)
pMTL-GCSY1	Shuttle vector (*E. coli* and *C. pasteurianum*) expressing glycine synthase (*gcvT* (Curi_c00740), *gcvH* (Curi_c00750), $gcvP_AP_B$ (Curi_c00760 and Curi_c00770) and *lpd* (Curi_c09790)) under fdx promotor originated from *Clostridium sporogenes* (Cm^R; ColE1 ori; pIM13 ori)	This study

TABLE 2 Primers used in this study for the construction of pMTL-GCSY1

Name	Sequence (5′–3′)
Lpd FOR[1]	AAATATACAAAGTAAATGACTCAAGGAATTTATGATGTTGTAGTTATAGGTG
Lpd REV[1]	ACGGGTGCTCGACATTTATTTTTTTGGCAGGTGTATACATTTATCAAATGTATCTGC
GCS FOR[2]	ACACAGGAAACAGCTATGGCTAAAAGAACAGCTCTTTATGAAATGCATAAAAAACAC
GcvT REV[2]	TTATTTTGATTTATTGTGTCTTTCTAAGAACTTTCTGCTTATAACTTTC
GcvH FOR[3]	AATAAATCAAAATAAATGAGCAAAATAGTAGAAGGATTATTATATTCAGAAGACCAC
GcvH REV[3,8,9]	TATATATCTATGCATTTATTCTGCACAGAATGCTTCGTATTTTGC
GcvP FOR[4]	ATGCATAGATATATACCTAACACTGATGCTGAG
GcvP REV[4]	TTACTTTGTATATTTTAGTATTAGATCTTTTGCCGCTTTAGCTTC
OEVec FOR[5]	ATGTCGAGCACCCGTTCTCG
OEVec REV[5]	AGCTGTTTCCTGTGTGAAATTGTTATGAG
SeqVector I FOR[6,7,8,9]	ACGCTTCCCGAAGGGAGAAAG
SeqOE REV[6]	ATATCTTTCTTTCATTAGATATGACGACAGGAAGAGTTTGTAGAAACG
SeqVector IV REV[7]	TGGCAGTTTATGGCGGGCGTC
GCVT I FOR[7]	AGAAGACTTAGTTGAATTCTTACCAACTCCAG
GCVT IV FOR[7]	ATGATGATTCAATTAAAGTTTGGGAAGCAG
	Description
1	PCR amplification of *lpd* (Curi_c09790)
2	PCR amplification of *gcvT* (Curi_c00740)
3	PCR amplification of *gcvH* (Curi_c00750)
4	PCR amplification of $gcvP_A$ (Curi_c00760) and $gcvP_B$ (Curi_c00770)
5	PCR amplification of pMTL85141-Cas9n vector backbone
6	Colony-PCR verification PCR after In-Fusion Cloning
7	Sanger Sequencing after In-Fusion Cloning
8	Colony-PCR verification after transformation into pFnuDIIMKn harboring *E. coli*
9	Verification PCR for uptake of pMTL-GCSY1 via re-extraction from *C. pasteurianum*

adapted from Biebl (2001) (K_2HPO_4, 0.5 g L^{-1}; KH_2PO_4, 0.5 g L^{-1}, $MgSO_4 \times 7H_2O$, 0.2 g L^{-1}; $(NH_4)_2SO_4$, 3 g L^{-1}; $CaCl_2 \times 2H_2O$, 0.02 g L^{-1}; resazurin (sodium salt), 2 mg L^{-1}; trace element solution SL7, 2 ml L^{-1}; cysteine × HCl × H_2O, 0.5 g L^{-1}) was supplemented with 2 g L^{-1} of $CaCO_3$, 5 g L^{-1} of yeast extract, 5 mg L^{-1} of $FeSO_4 \times 7H_2O$, 0–8 g L^{-1} of sodium formate and 50 g L^{-1} of glycerol or 15 g L^{-1} of glucose for serum bottle experiments. As inoculum for batch and continuous fermentation, the same Biebl medium without sodium formate was used. For the labeling experiment, concentrations of K_2HPO_4 and KH_2PO_4 were increased to 3 g L^{-1}, $CaCO_3$ was not included, yeast extract, ^{13}C sodium formate, and glucose were supplemented at 1 g L^{-1}, 6 g L^{-1}, and 6 g L^{-1}, respectively. All liquid medium for serum bottles were adjusted to pH 6.5 by titration with HCl and flushed with O_2-free N_2 for 20 min at 90°C before sterilization at 121°C. Agar plates with 2 × YTG medium were prepared with an additional 1.5% (w/v) agar, which was cultivated in anaerobic jars containing Oxoid AnaeroGen (Thermo Fisher Scientific). For the mutant strain harboring pMTL-GCSY1, thiamphenicol (Tm) was supplemented to a final concentration of 7–10 μg ml^{-1}.

^{13}C-labeling experiments were performed in 20 ml serum bottles with 5 ml working volume. Cultures grown on a 2 × YTG medium were pelleted by centrifugation and used as inoculate at a starting optical density (600 nm) of 0.15. After 43 h of incubation at 35°C, the cells were harvested and hydrolyzed as described by Zamboni et al. (2009). Batch fermentations were conducted in duplicates in 2 L bioreactors (Bioengineering AG) with a working volume of 1.5 L agitated at 300 rpm. Continuous fermentations were performed in a DASGIP Parallel Bioreactor System (DASGIP Eppendorf) in a 300 ml bioreactor with a working volume of 200 ml agitated at 150 rpm. All fermentations were performed at 35°C with pH-controlled at 6.0 through titration with 5 M KOH. The fermentation medium was composed of basal Biebl medium without $CaCO_3$, supplemented with yeast extract at 1 g L^{-1}, glycerol at 80 g L^{-1} (batch), glucose at 10 g L^{-1} (continuous culture), and sodium formate at 0–4 g L^{-1}

(continuous culture). After sterilization at 121°C, the reactors were flushed with N_2 until inoculation. $FeSO_4 \times 7H_2O$, cysteine × HCl × H_2O, and Tm for the mutant strain were added at 5 mg L^{-1} (batch) or 10 mg L^{-1} (continuous), 0.5 g $L^{-1,}$ and 7 μg ml^{-1}, respectively, shortly before inoculation.

2.4 | Electro-transformation of *C. pasteurianum*

For the electro-transformation of *C. pasteurianum* R525 strain, previously described protocols by Pyne et al. (2013) and Schmitz et al. (2019) were adapted. Briefly, an overnight culture was grown in 2 × YTG medium from a glycerol stock, and used to inoculate a pre-warmed fresh 2 × YTG medium. When an OD_{600} of approx. 0.45 was reached, the *C. pasteurianum* R525 culture was added with glycine (1.25% (w/v)) and sucrose (0.4 M), further incubated at 35°C for 3–4 h, before harvested and washed two times in an SMP buffer (sucrose, 270 mM; $MgCl_2$, 1 mM; Na_3PO_4, 5 mM; pH, 6.5). About 550 μl of the competent cell suspension was mixed with 30 μl ethanol and 86.5 μg extracted pMTL-GCSY1 (50 μL), which was in vivo methylated via pFnuDIIMKn (Pyne et al., 2013), electro-transformed (exp. pulse, 1.8 kV, 25 μF, ∞ Ω), recovered in a 2 × YTG medium supplemented with 0.2 M sucrose and selected on 2 × YTG agar plates with Tm. After 5 days, colonies were visible, which were re-streaked onto new 2 × YTG agar plates with Tm. After further incubation for 5 days, freshly grown colonies were picked and inoculated into 2 × YTG medium supplemented with Tm. Glycerol stocks were prepared from 50 h grown cultures. The successful transformation was verified by PCR using re-extracted plasmids from the selected *C. pasteurianum* strain.

2.5 | Analytical methods

Cell concentrations were measured turbidometrically at 600 nm and a previously determined conversion factor of 0.336 g L^{-1} cell dry weight per unit cell density (Groeger et al., 2017) was used to calculate cell dry weight. Soluble extracellular metabolites were measured via HPLC (KNAUER) on an Aminex HPX-87H column (300 × 7.8 mm; Bio-Rad) at 60°C, using 5 mM H_2SO_4 as mobile phase at a flow rate of 0.6 ml min^{-1}, and a refractive index detector and an ultraviolet detector. For fermentations, the off-gas flow rate was measured by an EL-FLOW flowmeter (Bronkhorst) and gas composition was determined using a Balzers Omnistar GSD 300 Mass Spectrometer (Pfeiffer Vacuum GmbH). For ^{13}C-labeling experiments, approx. 0.5 mg of dry biomass was used to prepare proteinogenic amino acids as described by Zamboni et al. (2009), including the hydrolysis of protein with 6 M HCl, and the derivatization of proteinogenic amino acids with N-terbutyldimethylsilyl-N-methyltrifluoroacetamide/terbutyldimethyl-chlorosilane. The measurement of isotopomer abundances of proteinogenic amino acids was performed on a gas chromatograph coupled to a mass spectrometer (GC/MS) (Agilent Technologies) using an Agilent HP5 ms column (30 m × 0.25 mm, 0.25 μm), with helium as carrier gas at a flow rate of 1 ml min^{-1}. The temperature profile was as following: 80°C held for 1 min, increase at 20°C min^{-1} to 120°C, increase at 4°C min^{-1} to 270°C, increase at 20°C min^{-1} to 290°C, and held for 2 min. Correction of the natural abundance of isotopes was performed using IsoCor v2 (Millard et al., 2019).

The maximum growth rate was calculated with linear fit tool via Origin 2020 (OriginLab). Further calculations were performed via Excel (Microsoft). For batch fermentations, averages of five sampling points from end-exponential phase were used for calculation. Carbon and electron recoveries as measure for analytical completeness were calculated according to Equations (1) and (2), respectively. The biomass composition of $C_4H_7O_2N$ with a molar mass of 101.1 g mol^{-1} (Biebl, 2001) was assumed. Loss of C1 carbons represents the carbon recovery in the form of CO_2 and formate. Substrate specific yields and carbon distributions from detected metabolites were calculated according to Equations (3) and (4), respectively.

$$r_{Carbon}(t) = \frac{\sum_{i=1} n_{C,i} M_i c_i(t)}{n_{C,Glycerol} M_{Glycerol} (c_{Glycerol}(t_0) - c_{Glycerol}(t))} \quad (1)$$

$$r_{e^-}(t) = \frac{\sum_{i=1} n_{e^-,i} M_i c_i(t)}{n_{e^-,Glycerol} M_{Glycerol} (c_{Glycerol}(t_0) - c_{Glycerol}(t))} \quad (2)$$

$$Y_i(t) = \frac{\sum_{i=1} (c_i(t) - c_i(t_0))}{c_{Glycerol}(t_0) - c_{Glycerol}(t)} \quad (3)$$

$$p_{C,i}(t) = \frac{n_{C,i} M_i c_i(t)}{\sum_{j=1} n_{C,j} M_j c_j(t)} \quad (4)$$

$$Q_i = M_i (c_i - c_{i,Feed}) V_R D \quad (5)$$

$$q_i = \frac{M_i (c_i - c_{i,Feed})}{c_{CDW}} D \quad (6)$$

$$r_{Carbon} = \frac{\sum_{i=1} n_{C,i} Q_i}{n_{C,Glucose} Q_{Glucose} + n_{C,Formate} Q_{Formate}} \quad (7)$$

$$r_{e^-} = \frac{\sum_{i=1} n_{e^-,i} Q_i}{n_{e^-,Glucose} Q_{Glucose} + n_{e^-,Formate} Q_{Formate}} \quad (8)$$

r_{Carbon}: carbon distribution, M_i: molar mass of compound i, $n_{C,i}$: number of carbons in compound i, c_i: concentration of compound i, r_{e^-}: electron recovery, $n_{e^-,i}$: total degree of reduction in compound i, Y_i: substrate-specific yield, $p_{C,i}$: carbon distribution of product i, Q_i: production/consumption rate, $c_{i,Feed}$: concentration of compound i in feed, V_R: reactor volume, D: dilution rate.

2.6 | Reverse transcription-polymerase chain reaction

C. pasteurianum R525 strain and pMTL-GCSY1 harboring mutant strain were grown in serum bottle (25 ml of modified Biebl medium supplemented with 15 g L^{-1} glucose and 1 g L^{-1} sodium formate) at 35°C and harvested after 22 and 25 h, respectively. Total RNA was extracted using Aurum Total RNA Mini Kit (Bio-Rad) with lysozyme purchased from Carl Roth (≥45,000 FIP U mg^{-1}). Reverse transcrip-

tion of RNA to cDNA was performed by using the reaction setup with gene-specific primers of iScript Select cDNA Synthesis Kit (Bio-Rad) including DNase I treatment. The manufacturer's instructions were followed for both kits. The obtained cDNA was qualitatively verified by CloneAmp HiFi PCR Premix and by using cDNA as a template. pMTL-GCSY1 was used as a positive control. As a negative control, water sample, cDNA of reverse-transcribed RNA from *C. pasteurianum* R525 strain with corresponding primers, and total RNA of the mutant strain were used as a template. Primers for reverse transcription PCR and the subsequent PCR for qualitative analysis are listed in Table S2, which were designed using Primer-BLAST (Ye et al., 2012).

2.7 | Genomic analysis methods

To find the presence of glycine cleavage system/glycine synthase proteins UniProtKB database (www.uniprot.org; The UniProt Consortium, 2019) was utilized for the search of specific conserved proteins or domains (Pfam; El-Gebali et al., 2019; Table S1).

3 | RESULTS AND DISCUSSION

3.1 | Introduction of glycine synthase into *C. pasteurianum*

Genes of the glycine synthase (glycine cleavage system) from the *gcv* cluster in *G. acidurici* (*gcvT*, *gcvH*, $gcvP_A$, and $gcvP_B$) and dihydrolipoamide dehydrogenase (*lpd*) were cloned into a previously constructed pMTL-based expression vector of pMTL85141-Cas9n (Schmitz et al., 2019). The resulting pMTL-GCSY1 plasmid was transformed into the *C. pasteurianum* R525 strain (termed WT), resulting in a *C. pasteurianum* mutant strain (termed as GCSY1) harboring the introduced glycine synthase. The successful plasmid uptake was verified by PCR after re-extraction from the GCSY1 strain. In addition, the heterologous expression of the genes was qualitatively confirmed by reverse transcription PCR (see Figure S1). Overall, a transformation efficiency of $(4.9 \pm 0.4) \times 10^{-1}$ transformants μg^{-1}_{DNA} ($n = 2$) was reached based on Tm selection. However, in comparison with previous reports of successful transformations with pMTL85141 (Heap et al., 2009) which reaches up to 10^5 transformants μg^{-1}_{DNA} (Grosse-Honebrink et al., 2017; Pyne et al., 2013), what we achieved was a six order of magnitude lower transformation efficiency. Since the number of plasmids during the transformation was not the limiting factor, we interpret that only a small proportion of cells were actually competent, supporting the hypothesis of Schmitz et al. (2019), Schwarz et al. (2017) and Grosse-Honebrink et al. (2017) that unknown barriers other than the restriction-modification system hinder foreign DNA transfer and the elevated competency as it was reported for R525, H1 and H3 strains was rather due to spontaneous and less controllable mutations.

3.2 | Metabolic and redox burdens led to secretion of 2-oxobutyrate and 3-hydroxypropionic aldehyde; formate as glycine synthase trigger

The GCSY1 strain showed deviations in growth pattern, secreted metabolites in serum bottle studies. When glycerol stocks of this strain were inoculated into 2 × YTG medium, both the lag-phase and the growth duration were prolonged in comparison with the WT strain from approx. 8–20 h and 16–40 h, respectively. Since the complex 2 × YTG medium is rich in nutrients the reason for the observed growth-inhibition was believed to be due to metabolic burden or instability caused by the introduction of glycine synthase, not the unavailability of certain nutrients in the medium. To further study the impact, pH-uncontrolled cultivations on glycerol in serum bottles with Biebl medium were performed with or without the supplementation of sodium formate and compared to the WT strain (see Figure 2a). The WT strain showed elevated growth inhibition with increasing sodium formate supplementation. Supplementation of formate to the culture of GCSY1 strain led to a nearly complete growth depletion, without apparent glycerol consumption. Thus, to identify the cause of growth inhibition of GCSY1 triggered by formate supplementation, the supernatant of culture broth was analyzed by HPLC.

First, the integration of glycine synthase into *C. pasteurianum* led to the formation of a metabolite, which was secreted into the culture medium and appeared as an unknown peak on the HPLC chromatogram. By checking the metabolic pathways that might be involved 2-oxobutyrate (2-OB) was identified, among others, as a possible candidate. This was then verified by spiking the samples with 2-OB standard, as well as by varying the HPLC condition to watch the retention time shift. 2-OB was never observed before in any previous works dealt with different strains of *C. pasteurianum*. However, 2-OB production ceased by repeated passaging into fresh complex medium or semi-synthetic medium, or in the progress of continuous fermentation, which suggests a metabolic adaptation of this microorganism.

2-OB can be formed as an intermediate in the amino acid metabolism and is linked to threonine conversion to isoleucine (Liu et al., 2016), or as a product of the degradation of cystathionine from the methionine cycle (Irmler et al., 2008) and propanoate metabolism (Srirangan et al., 2017). Although we are not able to clarify the exact origin of 2-OB secretion in this study, several possibilities exist regarding the connections of metabolic branches to the introduced glycine synthase (Figure 3a). First, glycine synthase may increase intracellular glycine level and reduce the need of glycine synthesis via threonine aldolase. To maintain the intracellular threonine level, more threonine is deaminated to 2-OB. Second, as one of the educts for the glycine synthase, the intracellular pool of 5,10-methylene-THF may be affected by the flux through glycine synthase. Subsequent fluxes are then adapted in the methionine and folate cycles, leading to an increased accumulation of cystathionine as the product of homocysteine demethylation. Degradation of cystathionine via cystathionine beta-lyase (*metC4*) may lead to 2-OB formation. Another possibility is revealed by the work of Nevin et al. (2011) who reported that microbial

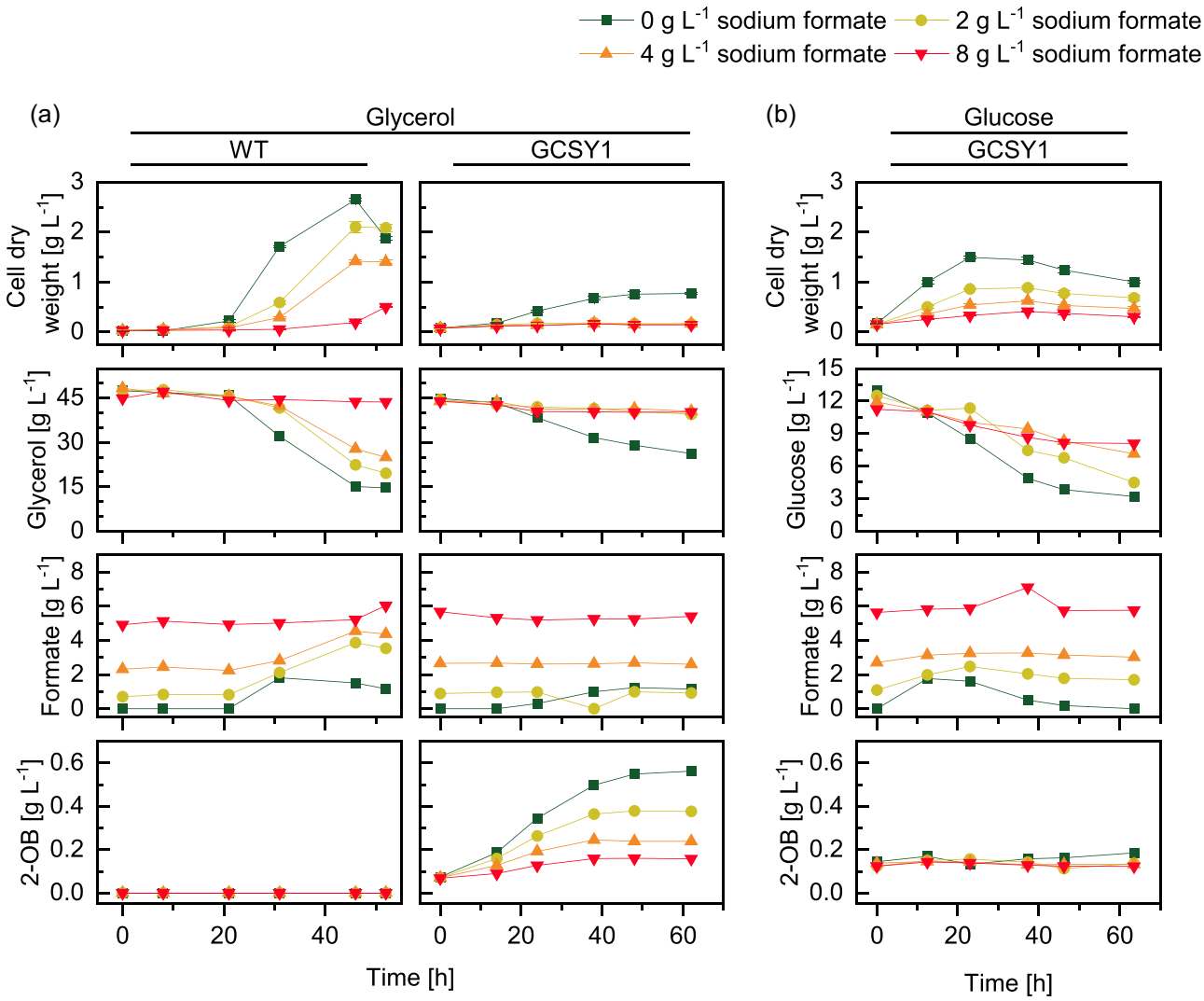

FIGURE 2 Changes in cell dry weight, glycerol, glucose, formate concentrations during pH-uncontrolled cultivation of *Clostridium pasteurianum* R525 (WT) and *C. pasteurianum* R525 glycine synthase mutant (GCSY1). Cultivations were performed in serum bottles with glycerol (a) or glucose (b) as substrates. Sodium formate was supplemented in varying concentrations (0, 2, 4, and 8 g L^{-1}), which corresponds to 0, 1.35, 2.71, and 5.41 g L^{-1} formate [Color figure can be viewed at wileyonlinelibrary.com]

electrosynthesis of *Clostridia* acetogens, such as *C. ljungdahlii* and *C. aceticum*, also led to the secretion of 2-OB in trace amounts, when CO_2 was fixated to acetate over the reductive acetyl-CoA pathway (rAP). Interestingly, these two *Clostridia* strains naturally harbor a glycine cleavage system (see Table S1). Assuming that a common causality for 2-OB secretion exists between the work of Nevin et al. (2011) and our observation, consumed electric current for acetogenesis in *C. ljungdhalii* and *C. aceticum* may pose a similar triggering effect as the redox shift of GCSY1 leading to 2-OB secretion. Supporting this hypothesis is the observation that the consumption of glycerol as a more reduced substrate instead of glucose by GCSY1 led to elevated 2-OB secretion in our study (see Figure 2b).

In addition to 2-OB, 3-hydroxypropionic aldehyde (3-HPA) was also found to be secreted into the medium in the culture of GCSY1 grown on glycerol but only in the presence of additionally supplemented formate. As shown in Figure S2, an asymmetrical HPLC-UV peak typical of 3-HPA in a dynamic equilibrium between its monomer, hydrate, and dimmer in aqueous solution was observed, as described in the HPLC analysis of 3-HPA by Burgé et al. (2015). Based on the phenomenon for several natural 1,3-PDO producers that 3-HPA accumulation is caused by an insufficient supply of reducing equivalents (NADH; Barbirato et al., 1998; Hao et al., 2008; Maervoet et al., 2016; Sauvageot et al., 2000; Wang et al., 2003) and absence of a direct metabolic link between 3-HPA and formate, we concluded a redox imbalance based on glycine synthase, which is triggered by formate addition.

Natively, the solventogenic pathway (see Figure 3b) of glycerol reduction over 3-HPA to 1,3-PDO is expected to be the major NADH oxidation route in glycerol fermentation of *C. pasteurinaum* which is crucial for redox homeostasis (Dabrock et al., 1992; Johnson & Rehmann, 2016; Pyne et al., 2016; Schmitz et al., 2019; Schwarz et al., 2017). 3-HPA accumulation was observed when formate was

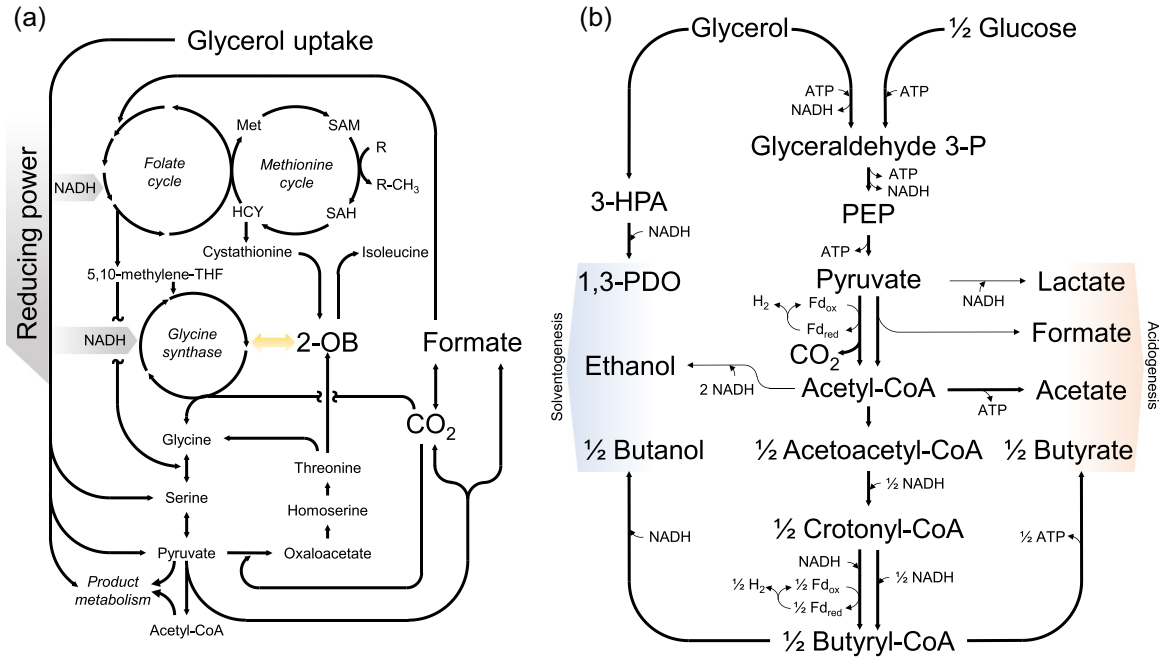

FIGURE 3 Interconnections among one-carbon metabolism with pathway branches shown toward 2-oxobutyrate and native acidogenesis and solventogenesis of *Clostridium pasteurianum* metabolism. (a) Methionine (Met), S-adenosylmethionine (SAM), S-adenosylhomocysteine (SAH), and homocysteine (HCY) from the methionine cycle are closely regulated and coupled with the folate cycle, which provides via THF activated C1 units for the reductive glycine pathway. Cystathionine is a degradation product of homocysteine that can be converted to 2-oxobutyrate (2-OB). In native *C. pasteurianum*, glycine is synthesized from threonine degradation. With the integration of glycine synthase system, an alternative glycine biosynthesis pathway is established. Threonine generated from pyruvate via oxaloacetate and homoserine is deaminated for the biosynthesis of isoleucine, yielding thereby 2-OB as an intermediate. The yellow arrow in both directions highlights the observed phenomenon: introduction of glycine synthase for the integration of reductive glycine pathway and elevation of reducing power (gray arrows) via utilization of glycerol by generating NADH for the reductive glycine pathway yields in 2-OB secretion. (b) Glycerol and glucose as the main carbon source of *C. pasteurianum* metabolism are converted to 1,3-PDO (from glycerol), ethanol, and butanol via solventogenesis, and lactate, formate, acetate, and butyrate via acidogenesis. Major C1 compounds (CO_2 and formate) is derived from the decarboxylation of pyruvate [Color figure can be viewed at wileyonlinelibrary.com]

added to the medium. Thus, we conclude that adding exogenous formate triggered reductive metabolic behavior, and cells counteracted by downregulating the reduction of 3-HPA to lower NADH oxidation. Since oxidation of formate to CO_2 via formate dehydrogenase or glycine cleavage reaction is expected to elevate reduction power (by recovering NAD(P)H), which promotes 3-HPA reduction to 1,3-PDO, the addition of exogenous formate appears not to induce CO_2 oxidation or glycine cleavage. Utilization of glucose instead of glycerol as the main carbon and energy source enabled a better growth of the GCSY1 strain despite formate addition (Figure 2b) due to the absence of 3-HPA biosynthesis route from glucose. Thus, for subsequent characterization of this strain, glycerol was used without exogenous formate addition, or glycerol was replaced by glucose, if sodium formate addition was desired.

3.3 | Native uptake of isotopically labeled formate

To characterize the formate-related metabolism of *C. pasteurianum*, ^{13}C-labeled formate was supplemented isotopomer distributions of the proteinogenic amino acids were profiled (Figure 4). For the WT strain, glycine should be synthesized via the native biosynthesis pathway from pyruvate either over serine or threonine due to the absence of glycine synthase (Figure 3a), and therefore, we expected only the appearance of M + 0 isotopomer for glycine (because the natural abundances of isotopes were subtracted). To our surprise, in the WT strain, glycine was found to have over 8% of M + 1 isotopomer (Figure 4b). This indicates that ^{13}C from labeled formate was incorporated into either the carboxyl or the aminomethyl group of glycine.

Based on this result and the study of Dainty and Peel (1970), we propose that a circular amino acid interconversion pathway exits in the native metabolism of *C. pasteurianum* as follows: C_3-central carbon metabolite (pyruvate and derivatives) ↔ oxaloacetate → aspartate → threonine → glycine ↔ serine ↔ C_3-central carbon metabolite (similar to the so-called serine-threonine-cycle; see Figure 4a). Considering the absence of native glycine synthase (glycine cleavage system) in the WT strain, the threonine aldolase reaction dissociating the third and fourth carbons and serine hydroxymethyltransferase cleaving the third carbon, M + 1 isotopomer of glycine indicates that first or second two carbons of C_3-central carbon metabolites must be originated from labeled formate (e.g.,

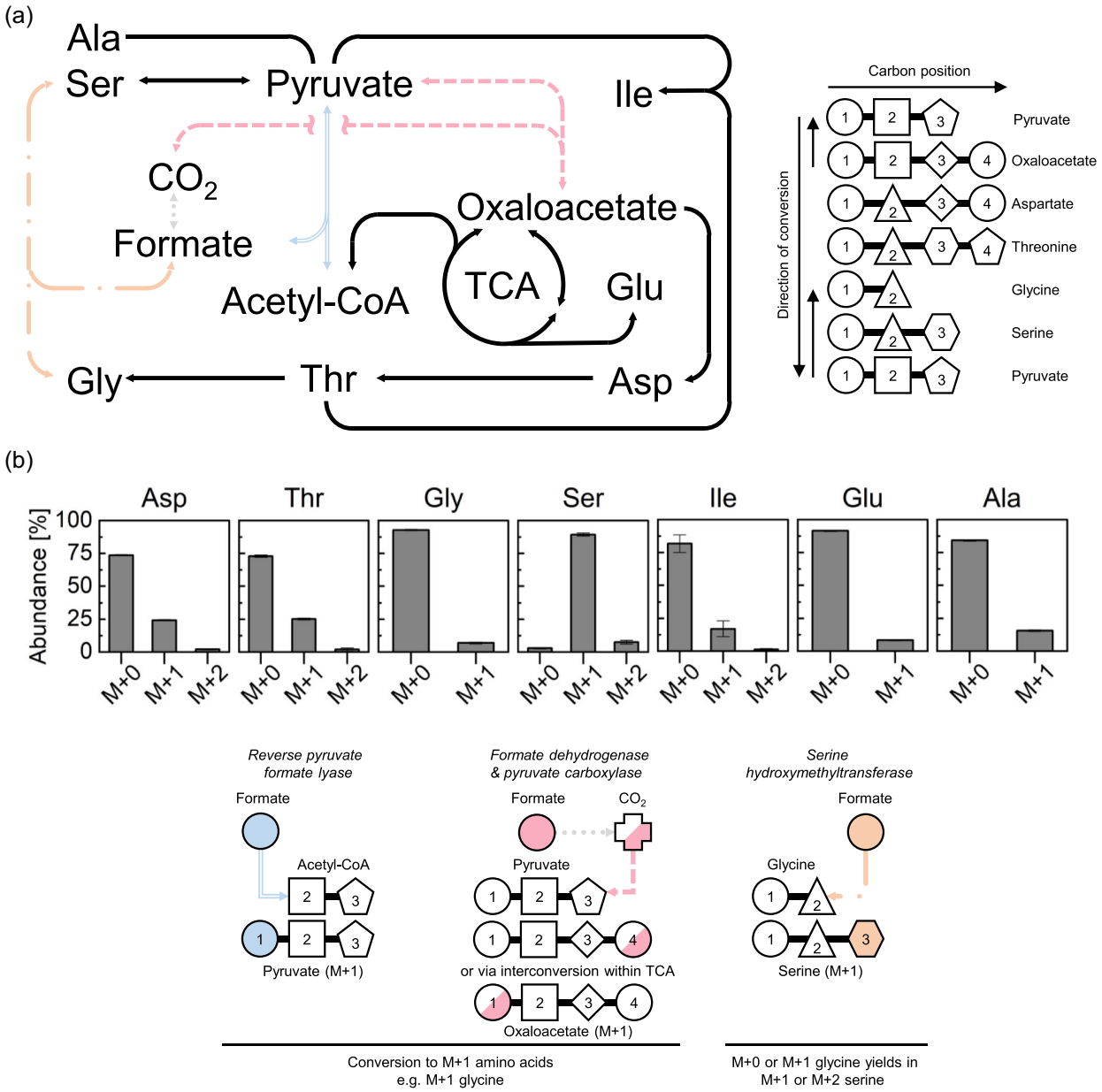

FIGURE 4 Distribution of assimilated ^{13}C-formate in *Clostridium pasteurianum* R525 (WT). (a) Metabolic scheme of amino acid conversions with numbered carbon positions passed on during the conversion. Colored arrows indicate fixation routes described in (c). Functional groups are represented as circle (carboxyl group), square (carbonyl group), pentagon (methyl group), rhombus (methylene bridge), triangle (aminomethyl group), hexagon (hydroxymethyl group), and cross (CO_2). (b) M + 0, M + 1, M + 2 abundances of glycine (Gly), serine (Ser), alanine (Ala), threonine (Thr), aspartate (Asp), isoleucine (Ile), and glutamate (Glu) of *C. pasteurianum* R525 (WT; $n = 5$). (c) Carbon pattern of different ^{13}C-formate fixation routes (from left to right): reverse pyruvate formate lyase based formate uptake (double-lined; blue), pyruvate carboxylase with interconversions to symmetrical TCA intermediates (dashed; pink), and serine hydroxymethyltransferase (dash-dotted; orange). Gray and dotted arrow indicates ^{13}C-labeled CO_2 from the partial oxidation of labeled formate via formate dehydrogenase [Color figure can be viewed at wileyonlinelibrary.com]

carboxyl or carbonyl group in pyruvate). We hypothesize a reversed pyruvate formate lyase reaction which yields in ^{13}C-labeling of the carboxyl group in pyruvate (see Figure 4c) as previously demonstrated in vitro for other *Clostridia* (Thauer et al., 1972) and applied in vivo in *E. coli* (Zelcbuch et al., 2016). Alternatively, fixation of CO_2 from oxidized ^{13}C-formate via pyruvate carboxylase as anaplerosis and interconversion within symmetrical TCA intermediates yields likewise in labeled pyruvate. However, the incompleteness of genes for the citrate cycle and unclear synthesis routes of TCA intermediates (Pyne et al., 2016) render a detailed investigation difficult. Nevertheless, both labeling patterns result in labeled central C_3 metabolite(s), which transfer labeled carbon to form glycine either over aspartate and threonine (with over 24% M + 1) or over serine. The unusually over 89% high M + 1 abundance and over 7%

abundance of M + 2 in serine are attributed to formate uptake via serine hydroxymethyltransferase from glycine (see Figure 4c) in addition to the canonical biosynthesis from labeled C_3 metabolite. Furthermore, alanine and glutamate synthesized from pyruvate were found to have approx. 15% and 7% M + 1 isotopomer, respectively.

Cultivating the GCSY1 mutant with exogenously added ^{13}C-formate, elevated acidogenesis in GCSY1 led to a drastic decrease of pH, despite increased phosphate buffer concentration in the medium was used. This induced early growth inhibition and partial sporulation of the cells. The resulting only 1.9-fold increase of the total biomass disqualified qualitative analysis of the functionality of glycine synthase in the GCSY1 mutant by using ^{13}C-labeled formate. Hence, an alternative approach was chosen to quantify the effect of glycine synthase on *C. pasteurianum*: since the costly usage of ^{13}C-labeled compounds can be only conducted in small mL-scales, we proceeded to scale-up the cultivation volumes enabling measurements of absolute concentrations of C1 compounds. Thus, batch fermentations in 1.5 L and continuous fermentations in 200 ml scales were performed to enhance the resolution of metabolic characterization. In addition, off-gas analysis was conducted to examine gaseous C1 production or consumption for GCSY1.

3.4 | Shift in solventogenesis and acidogenesis, reduction of carbon loss as C1 units without exogenous formate

Since formate and CO_2 are native by-products of *C. pasteurianum* metabolism, 1.5 L batch fermentations with glycerol as sole substrate (80 g L^{-1}) were conducted to analyze the impact of glycine synthase on natively synthesized C1 compounds (formate and CO_2; see Figure S3). Carbon recovery of approx. 95.3 ± 5.5% to 99.3 ± 0.9% and electron recovery from approx. 92.0 ± 5.4% to 103.0 ± 2.4% confirm that major metabolites were included in the analysis (Figure 5b). Since GCSY1 consumed less substrate, the following discussion is based on the distribution of carbon per unit of consumed glycerol.

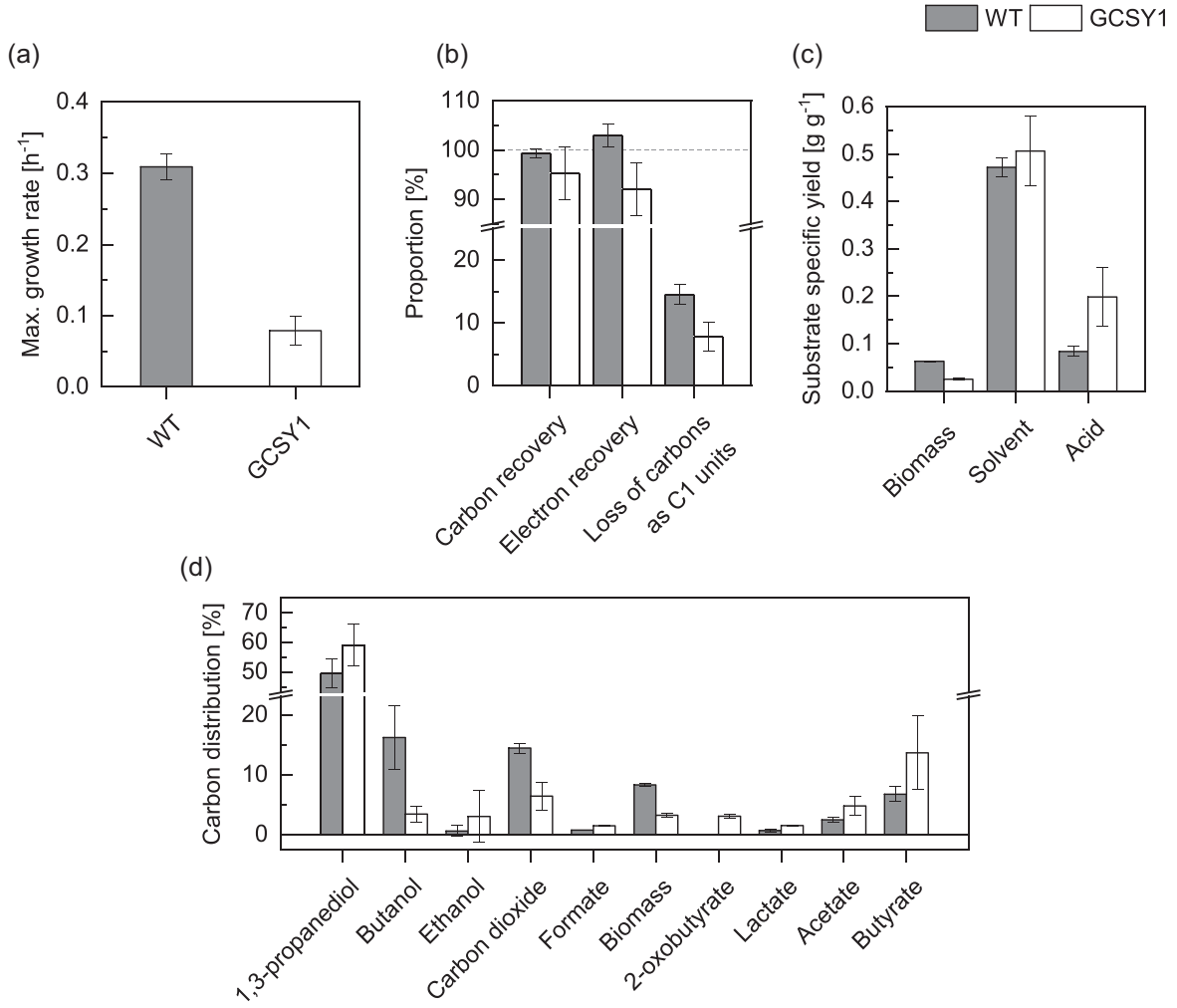

FIGURE 5 Analysis of batch fermentation data of *Clostridium pasteurianum* R525 (WT) and *C. pasteurianum* R525 glycine synthase mutant (GCSY1; $n = 2$). pH-controlled batch fermentations with glycerol (initial concentration 80 g L^{-1}) as the main carbon source were conducted in duplicates for both strains. The specific maximum growth rates were calculated from the growth curves of the early-exponential phase (a). Carbon and electron recoveries and proportion of carbon loss as C1 compounds (formate and CO_2) (b), substrate-specific yields (c), and carbon distributions (d) were calculated from an end-exponential phase of the batch fermentation

Shifts in the carbon fluxes were observed for GCSY1, which are attributed to glycine synthase introduction (Figure 5d): decreased carbon fluxes toward butanol (from 16.2 ± 5.4% to 3.5 ± 1.3%), carbon dioxide (from 14.5 ± 0.8% to 6.4 ± 2.3%) and biomass (from 8.3 ± 0.2% to 3.2 ± 0.3%), but increased carbon fluxes to acid production (from 10.7 ± 1.9% to 24.6 ± 8.1% for all detected acids), which is in agreement with substrate-specific yields as shown in Figure 5c. Metabolic burden via glycine synthase is observable by the decrease in the maximum growth rate from 0.309 ± 0.018 h^{-1} to 0.079 ± 0.002 h^{-1} (Figure 5a) and the decreased substrate-specific biomass yield from 63.15 ± 1.44 mg g^{-1} to 25.30 ± 2.37 mg g^{-1} as shown in Figure 5c. Similar to previously seen in serum bottle experiments, 2-OB secretion was observed (Figure S3), which accounted for up to 3.1 ± 0.4% of the carbon flux.

As the major impact of glycine synthase integration, carbon loss by CO_2 production from total consumed carbons was more than halved, despite the native formate uptake route. The alteration of native acidogenesis and solventogenesis was primarily observed for subsequent pathways of pyruvate: decreased butanol synthesis was observed, which results in lowered NADH oxidation, and carbon fluxes toward acid production in GCSY1 were more than doubled in comparison with WT. Elevated acetate and butyrate formation from glycerol (with 2 and 3 mol_{ATP} mol_{Acid}^{-1}, respectively) indicate elevated substrate-level phosphorylation. Overall, the metabolic impact of glycine synthase integration with additional ATP and NADH demand is in accordance with the elevated supply of ATP (acidogenesis) and the downregulation of competing for NADH oxidizing pathways (butanol). In conclusion, glycine synthase introduction led to reduced production of C1 units of approx. 46% in the GCSY1 strain compared to that of the WT strain. The overall metabolic burden or imbalance was manifested by decreased and slowed biomass formation. Further, this was accompanied by a carbon flux shift toward acidogenesis, resulting in over 2.3-fold increased substrate-specific yield, which poses an interesting strategy for bioprocesses for organic acid production (e.g., butyrate).

3.5 | Exogenous formate uptake with increasing formate supply

To analyze the ability of exogenous formate uptake and better comparability with the WT, glycerol was replaced by glucose (10 g L^{-1}), and substrate-limited continuous fermentation was performed at a dilution rate of 0.1 h^{-1} with 0, 1, 2, and 4 g L^{-1} sodium formate (see Figure S4). Interestingly, 2-OB secretion was not observable anymore as soon as the continuous operation mode was initiated. Thus, it appears that usage of more oxidized substrate in limited availability diminishes this metabolic imbalance as observed in batch fermentations with glycerol as the sole substrate. The continuous supply of 1 g L^{-1} yeast extract in the feed resulted in carbon and electron recoveries over 100% for all analyzed steady-state sampling points of WT and GCSY1 (see Figure 6a). The glucose-limited condition resulted in similar glucose consumption rates between WT and GCSY1 (between 1.050 ± 0.001 mmol h^{-1} and 1.094 ± 0.000 mmol h^{-1}) as shown in Figure 6c. While the biomass production rate for WT decreased by approx. 35% from 36.21 ± 1.28 mg h^{-1} with increasing sodium formate concentration, the GCSY1 strain showed higher tolerance with only a decrease of approx. 8% from 30.71 ± 0.29 mg h^{-1} (Figure 6d).

In regard to acidogenesis a tendency was observed: with increasing concentrations of sodium formate in the feed, the substrate-specific production rates of acids for WT were increased stepwise from 3.291 ± 0.137 mmol g^{-1} h^{-1} by approx. 40%, 98%, and 107%, at 1, 2, and 4 g L^{-1} sodium formate, respectively. For GCSY1, an increase of 22% from 4.032 ± 0.038 mmol g^{-1} h^{-1} was observed, when 1 g L^{-1} sodium formate was supplemented. However, a further increase in sodium formate did not result in an elevation of acidogenesis (see Figure 6e). As reported for *C. acetobutylicum* and *C. beijerinckii*, sodium formate supply in low concentration creates oxidative stress and leads to the so-called "acid crash" (Cho et al., 2012; Wang et al., 2011). The comparison of the specific acid production rate in regard to the biomass production rates (see Figure 6d) suggests elevated stress response in the WT strain due to increased supply of exogenous formate leading to increased ATP demand, which is compensated by elevated acidogenesis. In GCSY1, however, the increase of acidogenesis is confined despite the integration of glycine synthase. It appears in this context that the expected increase of ATP demand is negligible in comparison to the stress response related ATP demand as seen in WT. Solventogenesis was low for both strains and show no clear trends (see Figure 6f). This is conceivable, since glucose is less reduced than glycerol and solventogenesis should not be as dominant as that in glycerol fermentation for both strains.

The triggering effect of formate was most noticeable by production rates of C1 compounds: increased sodium formate supply increased gradually CO_2 production in WT from 3.894 ± 0.137 mmol g^{-1} h^{-1} to 7.223 ± 0.093 mmol g^{-1} h^{-1} and in GCSY1 from 3.976 ± 0.038 mmol g^{-1} h^{-1} to 5.757 ± 0.065 mmol g^{-1} h^{-1} (see Figure 7a). However, at approx. 24% and 20% lower CO_2 production was observed for GCSY1 at 2 and 4 g L^{-1} sodium formate concentration. Further, the elevation of exogenous formate led to its consumption by GCSY1. Specific consumption rates of 0.085 ± 0.068 mmol g^{-1} h^{-1} and 0.290 ± 0.016 mmol g^{-1} h^{-1} at 2 and 4 g L^{-1} sodium formate concentration, respectively, were observed as shown in Figure 7b, in contrast to increasing formate production rates in WT. In the discussed context, a consumption rate in the order of magnitude of 10^2 µmol g^{-1} h^{-1} may appear almost irrelevant, the resulting consumption was comprised of the consumption of exogenous formate added to the consumption of synthesized formate by its native metabolism. As shown by the specific C1 unit production rates depicted in Figure 7c, a reduction of up to 30% in total C1 production (at 2 and 4 g L^{-1} sodium formate in the feed) was observed. Furthermore, oxidation of formate to CO_2 and glycine cleavage can be excluded, since exogenous formate consumption did not lead toward elevated CO_2 production verifying the uptake and fixation of exogenous C1 compounds. It also implies the contrast of

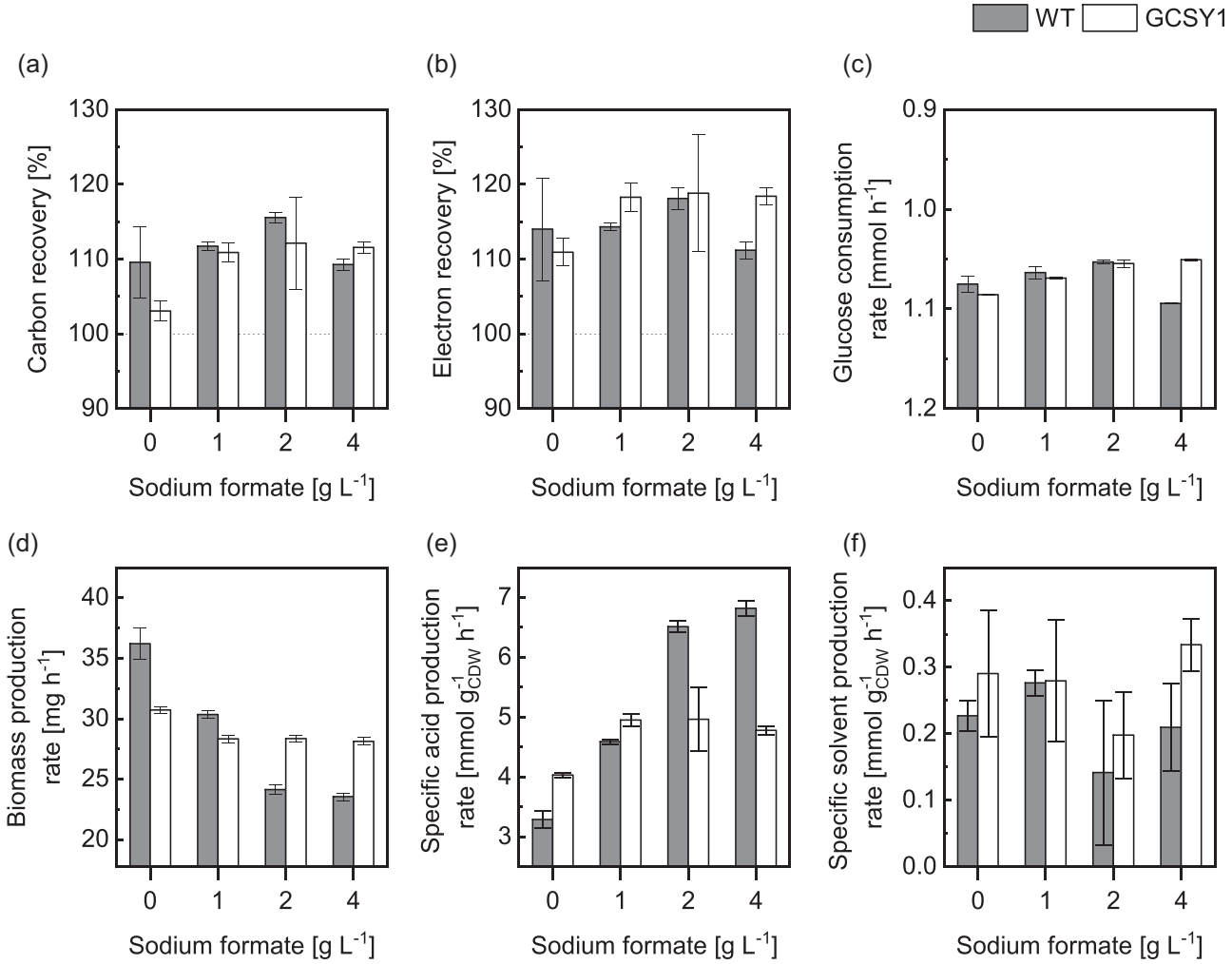

FIGURE 6 Analysis of continuous fermentation data of *Clostridium pasteurianum* R525 (WT) and *C. pasteurianum* R525 glycine synthase mutant (GCSY1; $n = 3$). Steady-state samples of pH-controlled continuous fermentation with glucose (10 g L^{-1}) and varying sodium formate concentrations are analyzed and shown as carbon (a), electron recoveries (b), glucose consumption (c), biomass production rates (d), specific acid (e), and solvent production rates (f)

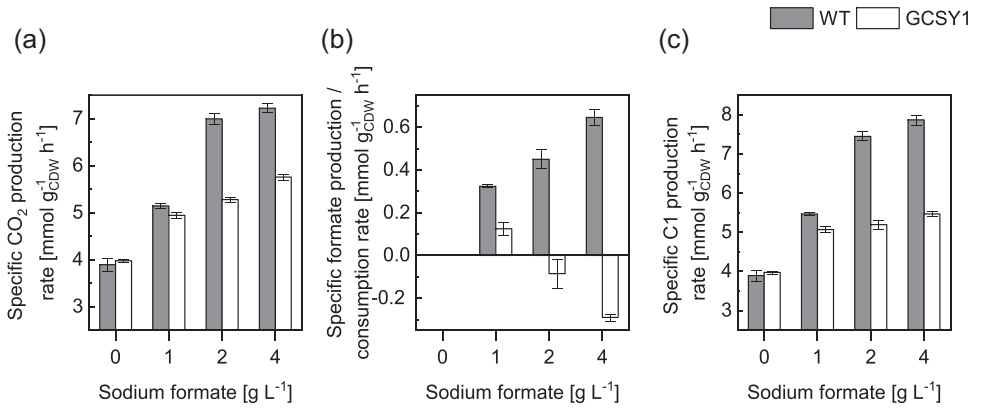

FIGURE 7 Specific C1 compound production and consumption rates from continuous fermentation of *Clostridium pasteurianum* R525 (WT) and *C. pasteurianum* R525 glycine synthase mutant (GCSY1; $n = 3$). Steady-state measurements of pH-controlled continuous fermentation with glucose (10 g L^{-1}) and varying sodium formate concentrations for WT and GCSY1 are compared for specific CO_2 (a), formate (b), and C1 (CO_2 and formate) production rates (c)

the presented approach to the engineering of aerobic microorganisms, where oxidation of formate and oxidative phosphorylation provide energy and reducing power (Bang & Lee, 2018; Yishai et al., 2018). It appears the additional burden for energy and reducing power was only compensated by lowered biomass production. This may pose a general constraint of this approach for C1 fixation toward valorized chemicals. However, it simultaneously demonstrates the ability to improve the overall carbon yield for the biosynthesis of chemicals through lowered production of biomass and CO_2. To pursue in-depth tracing of fixated C1 compounds, the growth inhibitory effect of glycine synthase needs to be addressed first by further engineering. Still, closed carbon and electron balances and uptake of C1 compounds implies the integration of fixated carbons into detected metabolites or biomass.

4 | CONCLUSION

For the first time, an artificial formate assimilation pathway was realized in a *Clostridia* bacterium by introducing glycine synthase of *G. acidurici* into *C. pasteurianum*. The impact of this pathway engineering for the cellular metabolism and native C1 biosynthesis was analyzed under the variation of substrate and cultivation conditions. The growth inhibitory effect of glycine synthase integration leading to early growth cessation disabled to definitively confirm glycine biosynthesis from ^{13}C-formate. However, up to 46% reduced native C1 compounds production and uptake of exogenous formate coupled with lowered CO_2 production in cultivation experiments verified the fixation of C1 compounds—solely as an outcome of glycine synthase integration. Unexpected 2-OB secretion and 3-HPA accumulation as metabolic responses toward integration of glycine synthase represent alterations of cellular, energy, and redox metabolism. The discussed cellular response provides insight into central metabolism and pinpoints to serious metabolic imbalances in *C. pasteurianum*, which may be also prevalent in other Clostridia lacking glycine synthase/cleavage system and represent essential engineering targets for further improvement on C1 fixation.

ACKNOWLEDGMENT

This study did not receive any specific grant from funding agencies in the public, commercial, or not-for-profit sectors. Open access funding enabled and organized by Projekt DEAL.

CONFLICT OF INTERESTS

The authors declare that there are no conflict of interests.

AUTHOR CONTRIBUTIONS

Yaeseong Hong: Conceptualization; methodology; software; validation; formal analysis; investigation; data curation; writing - original draft; review & editing; visualization. **Philipp Arbter**: Conceptualization; methodology; resources; writing - review & editing. **Wei Wang**: Conceptualization; methodology; writing - review & editing. **Lilian N. Rojas**: Methodology; validation; investigation. **An-Ping Zeng**: Conceptualization; supervision; writing - review & editing; funding acquisition.

DATA AVAILABILITY STATEMENT

Data sets related to this work can be found at Mendeley Data repository: Hong, Yaeseong (2020), "Introduction of glycine synthase enables uptake of exogenous formate and strongly impacts the metabolism in *Clostridium pasteurianum*," Mendeley Data, V2, https://dx.doi.org/10.17632/jmwxtrkj5x.2

ORCID

Yaeseong Hong http://orcid.org/0000-0002-5607-3618
Philipp Arbter http://orcid.org/0000-0002-5166-0303
An-Ping Zeng http://orcid.org/0000-0001-9768-7096

REFERENCES

Antoniewicz, M. R. (2019). Synthetic methylotrophy: Strategies to assimilate methanol for growth and chemicals production. *Current Opinion in Biotechnology*, *59*, 165–174. https://doi.org/10.1016/j.copbio.2019.07.001

Bang, J., Hwang, C. H., Ahn, J. H., Lee, J. A., & Lee, S. Y. (2020). *Escherichia coli* is engineered to grow on CO_2 and formic acid. *Nature Microbiology*, *5*(12), 1459–1463. https://doi.org/10.1038/s41564-020-00793-9

Bang, J., & Lee, S. Y. (2018). Assimilation of formic acid and CO_2 by engineered *Escherichia coli* equipped with reconstructed one-carbon assimilation pathways. *Proceedings of the National Academy of Sciences of the United States of America*, *115*(40), E9271–E9279. https://doi.org/10.1073/pnas.1810386115

Barbirato, F., Soucaille, P., Camarasa, C., & Bories, A. (1998). Uncoupled glycerol distribution as the origin of the accumulation of 3-hydroxypropionaldehyde during the fermentation of glycerol by *Enterobacter agglomerans* CNCM 1210. *Biotechnology and Bioengineering*, *58*(2–3), 303–305. https://doi.org/10.1002/(SICI)1097-0290(19980420)58:2/3<303::AID-BIT28>3.0.CO;2-B

Bar-Even, A. (2016). Formate assimilation: The metabolic architecture of natural and synthetic pathways. *Biochemistry*, *55*(28), 3851–3863. https://doi.org/10.1021/acs.biochem.6b00495

Bar-Even, A., Noor, E., Flamholz, A., & Milo, R. (2013). Design and analysis of metabolic pathways supporting formatotrophic growth for electricity-dependent cultivation of microbes. *Biochimica et Biophysica Acta*, *1827*(8–9), 1039–1047. https://doi.org/10.1016/j.bbabio.2012.10.013

Biebl, H. (2001). Fermentation of glycerol by *Clostridium pasteurianum*—Batch and continuous culture studies. *Journal of Industrial Microbiology & Biotechnology*, *27*(1), 18–26. https://doi.org/10.1038/sj.jim.7000155

Burgé, G., Flourat, A. L., Pollet, B., Spinnler, H. E., & Allais, F. (2015). 3-Hydroxypropionaldehyde (3-HPA) quantification by HPLC using a synthetic acrolein-free 3-hydroxypropionaldehyde system as analytical standard. *Royal Society of Chemistry Advances*, *5*(112), 92619–92627. https://doi.org/10.1039/C5RA18274C

Carlson, E. D., & Papoutsakis, E. T. (2017). Heterologous expression of the *Clostridium carboxidivorans* CO dehydrogenase alone or together with the acetyl coenzyme a synthase enables both reduction of CO_2 and oxidation of CO by *Clostridium acetobutylicum*. *Applied and Environmental Microbiology*, *83*(16), https://doi.org/10.1128/AEM.00829-17

Cho, D. H., Shin, S.-J., & Kim, Y. H. (2012). Effects of acetic and formic acid on ABE production by *Clostridium acetobutylicum* and *Clostridium beijerinckii*. *Biotechnology and Bioprocess Engineering*, *17*(2), 270–275. https://doi.org/10.1007/s12257-011-0498-4

Claassens, N. J., Bordanaba-Florit, G., Cotton, C. A. R., De Maria, A., Finger-Bou, M., Friedeheim, L., Giner-Laguarda, N., Munar-Palmer, M., Newell, W., Scarinci, G., Verbunt, J., de Vries, S. T., Yilmaz, S., & Bar-Even, A. (2020). Replacing the Calvin cycle with the reductive glycine pathway in *Cupriavidus necator*. *Metabolic Engineering*, *62*, 30–41. https://doi.org/10.1016/j.ymben.2020.08.004

Cotton, C. A., Claassens, N. J., Benito-Vaquerizo, S., & Bar-Even, A. (2019). Renewable methanol and formate as microbial feedstocks. *Current Opinion in Biotechnology*, *62*, 168–180. https://doi.org/10.1016/j.copbio.2019.10.002

Dabrock, B., Bahl, H., & Gottschalk, G. (1992). Parameters affecting solvent production by *Clostridium pasteurianum*. *Applied and Environmental Microbiology*, *58*(4), 1233–1239.

Dai, Z., Gu, H., Zhang, S., Xin, F., Zhang, W., Dong, W., Ma, J., Jia, H., & Jiang, M. (2017). Metabolic construction strategies for direct methanol utilization in *Saccharomyces cerevisiae*. *Bioresource Technology*, *245*(Pt B), 1407–1412. https://doi.org/10.1016/j.biortech.2017.05.100

Dainty, R. H., & Peel, J. L. (1970). Biosynthesis of amino acids in *Clostridium pasteurianum*. *The Biochemical Journal*, *117*(3), 573–584. https://doi.org/10.1042/bj1170573

El-Gebali, S., Mistry, J., Bateman, A., Eddy, S. R., Luciani, A., Potter, S. C., Qureshi, M., Richardson, L. J., Salazar, G. A., Smart, A., Sonnhammer, E. L. L., Hirsh, L., Paladin, L., Piovesan, D., Tosatto, S. C. E., & Finn, R. D. (2019). The Pfam protein families database in 2019. *Nucleic Acids Research*, *47*(D1), D427–D432. https://doi.org/10.1093/nar/gky995

Fast, A. G., & Papoutsakis, E. T. (2018). Functional expression of the *Clostridium ljungdahlii* acetyl-coenzyme a synthase in *Clostridium acetobutylicum* as demonstrated by a novel in vivo CO exchange activity en route to heterologous installation of a functional Wood-Ljungdahl pathway. *Applied and Environmental Microbiology*, *84*(7), https://doi.org/10.1128/AEM.02307-17

Gariboldi, R. T., & Drake, H. L. (1984). Glycine synthase of the purinolytic bacterium, *Clostridium acidiurici*. Purification of the glycine-CO_2 exchange system. *The Journal of Biological Chemistry*, *259*(10), 6085–6089.

Gassler, T., Sauer, M., Gasser, B., Egermeier, M., Troyer, C., Causon, T., Hann, S., Mattanovich, D., & Steiger, M. G. (2020). The industrial yeast *Pichia pastoris* is converted from a heterotroph into an autotroph capable of growth on CO_2. *Nature Biotechnology*, *38*(2), 210–216. https://doi.org/10.1038/s41587-019-0363-0

Gleizer, S., Ben-Nissan, R., Bar-On, Y. M., Antonovsky, N., Noor, E., Zohar, Y., Jona, G., Krieger, E., Shamshoum, M., Bar-Even, A., & Milo, R. (2019). Conversion of *Escherichia coli* to generate all biomass carbon from CO_2. *Cell*, *179*(6), 1255–1263. https://doi.org/10.1016/j.cell.2019.11.009

Gonzalez de la Cruz, J., Machens, F., Messerschmidt, K., & Bar-Even, A. (2019). Core catalysis of the reductive glycine pathway demonstrated in yeast. *American Chemical Society Synthetic Biology*, *8*(5), 911–917. https://doi.org/10.1021/acssynbio.8b00464

Groeger, C., Wang, W., Sabra, W., Utesch, T., & Zeng, A.-P. (2017). Metabolic and proteomic analyses of product selectivity and redox regulation in *Clostridium pasteurianum* grown on glycerol under varied iron availability. *Microbial Cell Factories*, *16*(1), 64. https://doi.org/10.1186/s12934-017-0678-9

Grosse-Honebrink, A., Schwarz, K. M., Wang, H., Minton, N. P., & Zhang, Y. (2017). Improving gene transfer in *Clostridium pasteurianum* through the isolation of rare hypertransformable variants. *Anaerobe*, *48*, 203–205. https://doi.org/10.1016/j.anaerobe.2017.09.001

Hao, J., Lin, R., Zheng, Z., Sun, Y., & Liu, D. (2008). 3-Hydroxypropionaldehyde guided glycerol feeding strategy in aerobic 1,3-propanediol production by *Klebsiella pneumoniae*. *Journal of Industrial Microbiology & Biotechnology*, *35*(12), 1615–1624. https://doi.org/10.1007/s10295-008-0405-y

Heap, J. T., Pennington, O. J., Cartman, S. T., & Minton, N. P. (2009). A modular system for *Clostridium* shuttle plasmids. *Journal of Microbiological Methods*, *78*(1), 79–85. https://doi.org/10.1016/j.mimet.2009.05.004

Hennig, G., Haupka, C., Brito, L. F., Rückert, C., Cahoreau, E., Heux, S., & Wendisch, V. F. (2020). Methanol-essential growth of *Corynebacterium glutamicum*: Adaptive laboratory evolution overcomes limitation due to methanethiol assimilation pathway. *International Journal of Molecular Sciences*, *21*(10), 3617. https://doi.org/10.3390/ijms21103617

Irmler, S., Raboud, S., Beisert, B., Rauhut, D., & Berthoud, H. (2008). Cloning and characterization of two *Lactobacillus casei* genes encoding a cystathionine lyase. *Applied and Environmental Microbiology*, *74*(1), 99–106. https://doi.org/10.1128/AEM.00745-07

Johnson, E. E., & Rehmann, L. (2016). The role of 1,3-propanediol production in fermentation of glycerol by *Clostridium pasteurianum*. *Bioresource Technology*, *209*, 1–7. https://doi.org/10.1016/j.biortech.2016.02.088

Kikuchi, G., Motokawa, Y., Yoshida, T., & Hiraga, K. (2008). Glycine cleavage system: Reaction mechanism, physiological significance, and hyperglycinemia. *Proceedings of the Japan Academy. Series B, Physical and Biological Sciences*, *84*(7), 246–263. https://doi.org/10.2183/pjab.84.246

Liu, Y., Li, Y., & Wang, X. (2016). Acetohydroxyacid synthases: Evolution, structure, and function. *Applied Microbiology and Biotechnology*, *100*(20), 8633–8649. https://doi.org/10.1007/s00253-016-7809-9

Maervoet, V. E. T., Maeseneire, S. L., de, Avci, F. G., Beauprez, J., Soetaert, W. K., & de Mey, M. (2016). High yield 1,3-propanediol production by rational engineering of the 3-hydroxypropionaldehyde bottleneck in *Citrobacter werkmanii*. *Microbial Cell Factories*, *15*, 23. https://doi.org/10.1186/s12934-016-0421-y

Mao, W., Yuan, Q., Qi, H., Wang, Z., Ma, H., & Chen, T. (2020). Recent progress in metabolic engineering of microbial formate assimilation. *Applied Microbiology and Biotechnology*, *104*(16), 6905–6917. https://doi.org/10.1007/s00253-020-10725-6

Millard, P., Delépine, B., Guionnet, M., Heuillet, M., Bellvert, F., & Létisse, F. (2019). Isocor: Isotope correction for high-resolution MS labeling experiments. *Bioinformatics*, *35*(21), 4484–4487. https://doi.org/10.1093/bioinformatics/btz209

Nevin, K. P., Hensley, S. A., Franks, A. E., Summers, Z. M., Ou, J., Woodard, T. L., Snoeyenbos-West, O. L., & Lovley, D. R. (2011). Electrosynthesis of organic compounds from carbon dioxide is catalyzed by a diversity of acetogenic microorganisms. *Applied and Environmental Microbiology*, *77*(9), 2882–2886. https://doi.org/10.1128/AEM.02642-10

Pandit, A. V., Srinivasan, S., & Mahadevan, R. (2017). Redesigning metabolism based on orthogonality principles. *Nature Communications*, *8*, 15188. https://doi.org/10.1038/ncomms15188

Poehlein, A., Yutin, N., Daniel, R., & Galperin, M. Y. (2017). Proposal for the reclassification of obligately purine-fermenting bacteria *Clostridium acidurici* (Barker 1938) and *Clostridium purinilyticum* (Dürre et al. 1981) as *Gottschalkia acidurici* gen. nov. comb. nov. and *Gottschalkiapurinilytica* comb. nov. and of *Eubacterium angustum* (Beuscher and Andreesen 1985) as *Andreesenia angusta* gen. nov. comb. nov. in the family *Gottschalkiaceae* fam. nov. *International Journal of Systematic and Evolutionary Microbiology*, *67*(8), 2711–2719. https://doi.org/10.1099/ijsem.0.002008

Pyne, M. E., Liu, X., Moo-Young, M., Chung, D. A., & Chou, C. P. (2016). Genome-directed analysis of prophage excision, host defence systems, and central fermentative metabolism in *Clostridium pasteurianum*. *Scientific Reports*, *6*, 26228. https://doi.org/10.1038/srep26228

Pyne, M. E., Moo-Young, M., Chung, D. A., & Chou, C. P. (2013). Development of an electrotransformation protocol for genetic

manipulation of *Clostridium pasteurianum*. *Biotechnology for Biofuels*, *6*(1), 50. https://doi.org/10.1186/1754-6834-6-50

Pyne, M. E., Sokolenko, S., Liu, X., Srirangan, K., Bruder, M. R., Aucoin, M. G., Moo-Young, M., Chung, D. A., & Chou, C. P. (2016). Disruption of the reductive 1,3-propanediol pathway triggers production of 1,2-propanediol for sustained glycerol fermentation by *Clostridium pasteurianum*. *Applied and Environmental Microbiology*, *82*(17), 5375–5388. https://doi.org/10.1128/AEM.01354-16

Sauvageot, N., Gouffi, K., Laplace, J.-M., & Auffray, Y. (2000). Glycerol metabolism in *Lactobacillus collinoides*: Production of 3-hydroxypropionaldehyde, a precursor of acrolein. *International Journal of Food Microbiology*, *55*(1–3), 167–170. https://doi.org/10.1016/S0168-1605(00)00191-4

Schmitz, R., Sabra, W., Arbter, P., Hong, Y., Utesch, T., & Zeng, A.-P. (2019). Improved electrocompetence and metabolic engineering of *Clostridium pasteurianum* reveals a new regulation pattern of glycerol fermentation. *Engineering in Life Sciences*, *19*(6), 412–422. https://doi.org/10.1002/elsc.201800118

Schwarz, K. M., Grosse-Honebrink, A., Derecka, K., Rotta, C., Zhang, Y., & Minton, N. P. (2017). Towards improved butanol production through targeted genetic modification of *Clostridium pasteurianum*. *Metabolic Engineering*, *40*, 124–137. https://doi.org/10.1016/j.ymben.2017.01.009

Srirangan, K., Bruder, M., Akawi, L., Miscevic, D., Kilpatrick, S., Moo-Young, M., & Chou, C. P. (2017). Recent advances in engineering propionyl-CoA metabolism for microbial production of value-added chemicals and biofuels. *Critical Reviews in Biotechnology*, *37*(6), 701–722. https://doi.org/10.1080/07388551.2016.1216391

Sánchez-Andrea, I., Guedes, I. A., Hornung, B., Boeren, S., Lawson, C. E., Sousa, D. Z., Bar-Even, A., Claassens, N. J., & Stams, A. J. M. (2020). The reductive glycine pathway allows autotrophic growth of *Desulfovibrio desulfuricans*. *Nature Communications*, *11*(1), 5090. https://doi.org/10.1038/s41467-020-18906-7

Thauer, R. K., Kirchniawy, F. H., & Jungermann, K. A. (1972). Properties and function of the pyruvate-formate-lyase reaction in clostridiae. *European Journal of Biochemistry*, *27*(2), 282–290. https://doi.org/10.1111/j.1432-1033.1972.tb01837.x

The UniProt Consortium. (2019). Uniprot: A worldwide hub of protein knowledge. *Nucleic Acids Research*, *47*(D1), D506–D515. https://doi.org/10.1093/nar/gky1049

Tuyishime, P., & Sinumvayo, J. P. (2020). Novel outlook in engineering synthetic methylotrophs and formatotrophs: A course for advancing C1-based chemicals production. *World Journal of Microbiology & Biotechnology*, *36*(8), 118. https://doi.org/10.1007/s11274-020-02899-y

Tuyishime, P., Wang, Y., Fan, L., Zhang, Q., Li, Q., Zheng, P., Sun, J., & Ma, Y. (2018). Engineering Corynebacterium glutamicum for methanol-dependent growth and glutamate production. *Metabolic Engineering*, *49*, 220–231. https://doi.org/10.1016/j.ymben.2018.07.011

Waber, L. J., & Wood, H. G. (1979). Mechanism of acetate synthesis from CO_2 by *Clostridium acidiurici*. *Journal of Bacteriology*, *140*(2), 468–478.

Wang, S., Zhang, Y., Dong, H., Mao, S., Zhu, Y., Wang, R., Luan, G., & Li, Y. (2011). Formic acid triggers the "Acid Crash" of acetone-butanol-ethanol fermentation by *Clostridium acetobutylicum*. *Applied and Environmental Microbiology*, *77*(5), 1674–1680. https://doi.org/10.1128/AEM.01835-10

Wang, W., Sun, J., Hartlep, M., Deckwer, W.-D., & Zeng, A.-P. (2003). Combined use of proteomic analysis and enzyme activity assays for metabolic pathway analysis of glycerol fermentation by *Klebsiella pneumoniae*. *Biotechnology and Bioengineering*, *83*(5), 525–536. https://doi.org/10.1002/bit.10701

Witthoff, S., Schmitz, K., Niedenführ, S., Nöh, K., Noack, S., Bott, M., & Marienhagen, J. (2015). Metabolic engineering of Corynebacterium glutamicum for methanol metabolism. *Applied and Environmental Microbiology*, *81*(6), 2215–2225. https://doi.org/10.1128/AEM.03110-14

Ye, J., Coulouris, G., Zaretskaya, I., Cutcutache, I., Rozen, S., & Madden, T. L. (2012). Primer-BLAST: A tool to design target-specific primers for polymerase chain reaction. *BMC Bioinformatics*, *13*, 134. https://doi.org/10.1186/1471-2105-13-134

Yishai, O., Bouzon, M., Döring, V., & Bar-Even, A. (2018). In vivo assimilation of one-carbon via a synthetic reductive glycine pathway in *Escherichia coli*. *American Chemical Society Synthetic Biology*, *7*(9), 2023–2028. https://doi.org/10.1021/acssynbio.8b00131

Zamboni, N., Fendt, S.-M., Rühl, M., & Sauer, U. (2009). (13)C-based metabolic flux analysis. *Nature Protocols*, *4*(6), 878–892. https://doi.org/10.1038/nprot.2009.58

Zelcbuch, L., Lindner, S. N., Zegman, Y., Vainberg Slutskin, I., Antonovsky, N., Gleizer, S., Milo, R., & Bar-Even, A. (2016). Pyruvate formate-lyase enables efficient growth of *Escherichia coli* on acetate and formate. *Biochemistry*, *55*(17), 2423–2426. https://doi.org/10.1021/acs.biochem.6b00184

SUPPORTING INFORMATION

Additional Supporting Information may be found online in the supporting information tab for this article.

How to cite this article: Hong Y, Arbter P, Wang W, Rojas LN, Zeng A-P. Introduction of glycine synthase enables uptake of exogenous formate and strongly impacts the metabolism in *Clostridium pasteurianum*. *Biotechnology and Bioengineering*. 2021;118:1366–1380. https://doi.org/10.1002/bit.27658